JOURNAL OF MORPHOLOGY 269:1041–1055 (2008)

Functional Morphology of the Feeding Apparatus, Feeding Constraints, and Suction Performance in the Nurse Shark *Ginglymostoma cirratum*

Philip J. Motta,[1]* Robert E. Hueter,[2] Timothy C. Tricas,[3] Adam P. Summers,[4] Daniel R. Huber,[5] Dayv Lowry,[6] Kyle R. Mara,[1] Michael P. Matott,[7] Lisa B. Whitenack,[1] and Alpa P. Wintzer[8]

[1]*Department of Biology, University of South Florida, Tampa, Florida 33620*
[2]*Center for Shark Research, Mote Marine Laboratory, Sarasota, Florida 34236*
[3]*Department of Zoology and Hawaii Institute of Marine Biology, University of Hawaii at Manoa, Honolulu, Hawaii 96822*
[4]*Department of Ecology and Evolutionary Biology, University of California Irvine, Irvine, California 92697*
[5]*Department of Biology, University of Tampa, Tampa, Florida 33606*
[6]*Washington Department of Fish and Wildlife, Point Whitney Shellfish Laboratory, Brinnon, Washington 98320*
[7]*Department of Molecular Pharmacology and Physiology, University of South Florida, Tampa, Florida 33620*
[8]*Department of Wildlife, Fish and Conservation Biology, University of California Davis, Davis, California 95616*

ABSTRACT The nurse shark, *Ginglymostoma cirratum*, is an obligate suction feeder that preys on benthic invertebrates and fish. Its cranial morphology exhibits a suite of structural and functional modifications that facilitate this mode of prey capture. During suction-feeding, subambient pressure is generated by the ventral expansion of the hyoid apparatus and the floor of its buccopharyngeal cavity. As in suction-feeding bony fishes, the nurse shark exhibits expansive, compressive, and recovery kinematic phases that produce posterior-directed water flow through the buccopharyngeal cavity. However, there is generally neither a preparatory phase nor cranial elevation. Suction is generated by the rapid depression of the buccopharyngeal floor by the coracoarcualis, coracohyoideus, and coracobranchiales muscles. Because the hyoid arch of *G. cirratum* is loosely connected to the mandible, contraction of the rectus cervicis muscle group can greatly depress the floor of the buccopharyngeal cavity below the depressed mandible, resulting in large volumetric expansion. Suction pressures in the nurse shark vary greatly, but include the greatest subambient pressures reported for an aquatic-feeding vertebrate. Maximum suction pressure does not appear to be related to shark size, but is correlated with the rate of buccopharyngeal expansion. As in suction-feeding bony fishes, suction in the nurse shark is only effective within approximately 3 cm in front of the mouth. The foraging behavior of this shark is most likely constrained to ambushing or stalking due to the exponential decay of effective suction in front of the mouth. Prey capture may be facilitated by foraging within reef confines and close to the substrate, which can enhance the effective suction distance, or by foraging at night when it can more closely approach prey. J. Morphol. 269:1041–1055, 2008.

KEY WORDS: Elasmobranchii; muscles; jaw; biomechanics; anatomy; suction feeding

Aquatic vertebrates are challenged with capturing prey under a myriad of circumstances. Prey may be suspended in the water column, buried in or attached to the substrate, elusive or stationary, and even hidden within crevices. Inertial suction-feeding is the primary method by which aquatic vertebrates capture this prey and it is the primitive method for bony fishes (Lauder, 1985). In contrast, based on the anatomy of the jaws, teeth, and suspensory mechanism, ram feeding and biting appear to be the predominant and ancestral mode of prey capture in elasmobranchs, with suction feeding evolving in numerous lineages of benthic sharks and rays, including the Heterodontiformes (horn sharks), Orectolobiformes (carpet sharks), Carcharhiniformes (ground sharks), Squaliformes (dogfish sharks), and batoids (rays). The former two groups include some of the most specialized obligate suction feeders (Motta et al., 2002; Wilga et al., 2007).

The bony fish feeding mechanism differs from that of sharks by having a greater number of moveable elements, greater lateral expansion during suction generation, a bony operculum and a bipartite upper jaw comprising a premaxilla and maxilla as opposed to the single palatoquadrate cartilage (Motta, 2004; Westneat, 2006; Wilga, 2008). In bony fishes, suction-feeding is dependent on a rapid series of kinematic events that include cranial elevation, abduction of the operculum and

Contract grant sponsor: National Science Foundation; Contract grant numbers: DEB 9117371, IBN 9807863; Contract grant sponsor: The Porter Family Foundation.

*Correspondence to: Philip J. Motta, Department of Biology, University of South Florida, 4202 East Fowler Avenue, Tampa, FL 33620. E-mail: motta@cas.usf.edu

Published online 12 May 2008 in
Wiley InterScience (www.interscience.wiley.com)
DOI: 10.1002/jmor.10626

suspensorium, mandible depression, upper jaw protrusion, and hyoid depression (Lauder, 1985; Westneat, 2006). The velocity of water flow into the mouth is related to the rate of buccal expansion and diminishes rapidly with distance from the mouth. Consequently, the maximum distance water may be sucked in by bony fish is approximately one mouth width or 3 cm (Muller et al., 1982; Van Leeuwen and Muller, 1984; Svanback et al., 2002). In suction-feeding sharks, anatomical differences in the feeding apparatus result in functional differences. Rapid buccopharyngeal expansion results from depression of the mandible, hyoid, and branchial arches. Cranial elevation and upper jaw protrusion play little or no role in volume expansion. In contrast to bony fishes where the hyoid cavity expands ventrally and laterally during suction feeding, the hyoid arch of sharks expands ventrally but compresses laterally during suction feeding. In addition, the lack of an operculum in sharks should preclude any significant generation of suction pressure by lateral expansion of the pharyngeal chamber, although slight subambient pressure has been recorded in the parabranchial chamber during respiration (Ferry-Graham, 1999; Edmonds et al., 2001; Motta et al., 2002; Matott et al., 2005; Huber et al., 2006; Lowry and Motta, 2007a; Wilga et al., 2007; Wilga, 2008). For small sharks at least, it appears that effective suction distance is similarly restricted to distances of approximately 3 cm because of hydrodynamic constraints (Wilga et al., 2007).

The orectolobiform sharks, which include the carpet, blind, nurse, wobbegong, bamboo, zebra, and whale sharks (Shirai, 1996), include many specialized suction feeders as evidenced by their anatomy and feeding kinematics (Moss, 1977; Wu, 1994; Motta et al., 2002; Lowry and Motta, 2007a). The nurse shark, *Ginglymostoma cirratum* is an obligate suction-feeding shark that grows to 300 cm TL (Compagno et al., 2005). During suction capture this shark displays little modulation in its prey capture kinematics or motor pattern (Motta et al., 2002; Robinson and Motta, 2002; Matott et al., 2005). This species is common in shallow tropical and subtropical waters throughout the northwest Atlantic Ocean including the West Indies and south Florida, where it feeds on small fishes and crustaceans (Gudger, 1921; Bigelow and Schroeder, 1948; Castro, 2000; Compagno, 2001). *Ginglymostoma cirratum* exhibits a suite of anatomical and behavioral specializations for suction-feeding that include rapid buccopharyngeal expansion, the formation of a small anteriorly directed mouth that is approximately round and laterally enclosed by modified and reinforced labial cartilages, small teeth, buccal valves to prevent the back-flow of water out the mouth, and purportedly hypertrophied jaw abductor muscles (Moss, 1965, 1977; Motta and Wilga, 1999; Motta et al., 2002; Matott et al., 2005). Preliminary performance measurements indicate that suction pressure generated during feeding by *G. cirratum* approaches 1 atm or −94 kPa (Tanaka, 1973).

There is an extensive literature on the biomechanics, kinematics and performance of suction feeding in bony fishes. However, studies of suction-feeding in elasmobranchs are confined principally to kinematics of select species including *Ginglymostoma cirratum* (Wu, 1994; Motta et al., 2002; Matott et al., 2005), spotted wobbegong *Orectolobus maculatus* (Wu, 1994), horn shark *Heterodontus francisci* (Edmonds et al., 2001), whitespotted bambooshark *Chiloscyllium plagiosum* (Nauwelaerts et al., 2006; Lowry and Motta, 2007a; Wilga et al., 2007; Ramsay and Wilga, 2008), spiny dogfish *Squalus acanthias* (Wilga and Motta, 1998), leopard shark *Triakis semifasciata* (Ferry-Graham, 1998; Lowry et al., 2007), lesser electric ray *Narcine brasiliensis* (Dean and Motta, 2004a,b), and cownose ray *Rhinoptera bonasus* (Sasko et al., 2006). Suction performance and its ecological significance has only been investigated in a few of these elasmobranchs (Sasko et al., 2006; Lowry and Motta, 2007b; Wilga et al., 2007; Ramsay and Wilga, 2008; Wilga, 2008). Therefore, the goals of this study were to: 1) investigate the functional morphology of suction-feeding in *G. cirratum* using anatomy, electromyography, and high-speed video; 2) quantify suction performance at two locations in the buccopharyngeal cavity; 3) determine the scaling of suction performance across a range of shark sizes; and 4) relate cranial morphology and suction performance of the nurse shark to feeding ecology and diet.

MATERIALS AND METHODS

Anatomy

To complement the anatomical descriptions of Motta and Wilga (1999), three partially dissected *Ginglymostoma cirratum* (101, 103, and 172 cm TL) specimens were manually manipulated to try and relate the electromyographic (EMG) motor patterns to kinesis of the feeding apparatus. Position of the elements during manipulation was based on the kinematic analysis of *G. cirratum* (Motta et al., 2002). All animals in this study were collected in Florida Bay north of the Florida Keys and treated in accordance with University of South Florida and Mote Marine Laboratory Institutional Care and Use Committee Guidelines (protocols 91.014, 1558, 1734, and 2046).

Computed Tomography

A series of images were taken of two fresh male specimens of *Ginglymostoma cirratum* (123 and 57 cm TL) with a Siemens DRH Computed Tomography scanner (Motta and Wilga, 1999). Images were taken of the smaller shark with the mouth in the closed, relaxed position, and of the larger shark with the mouth maximally open, labial cartilages extended, and palatoquadrate cartilage mostly protruded, indicating the position of the elements during jaw protrusion and adduction (Motta et al., 2002; Ramsay and Wilga, 2007). Imaging was performed in the transverse plane from the rostral margin of the head to the caudal

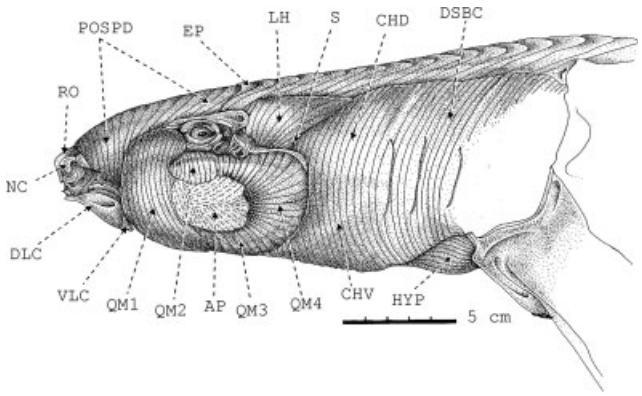

Fig. 1. Left lateral view of the head of a 97 cm TL male *Ginglymostoma cirratum* with the skin removed and the muscle fiber direction indicated. Myosepta of the epaxialis are indicated without fiber direction. AP, aponeurosis over QM2 and QM4; CHD, constrictor hyoideus dorsalis; CHV, constrictor hyoideus ventralis; DLC, dorsal labial cartilage; DSBC, dorsal superficial branchial constrictor; EP, epaxialis; HYP, hypaxialis; LH, levator hyomandibularis; NC, nasal capsule; POSPD, superficial head of posterior division of preorbitalis; QM1, quadratomandibularis division 1; QM2, quadratomandibularis division 2; QM3, quadratomandibularis division 3; QM4, quadratomandibularis division 4; RO, rostral cartilage; S, spiracle; VLC, ventral labial cartilage. (Reproduced from Motta and Wilga, J Morphol, 1999, 249, 1–29, © Wiley-Liss, a subsidiary of John Wiley and Sons).

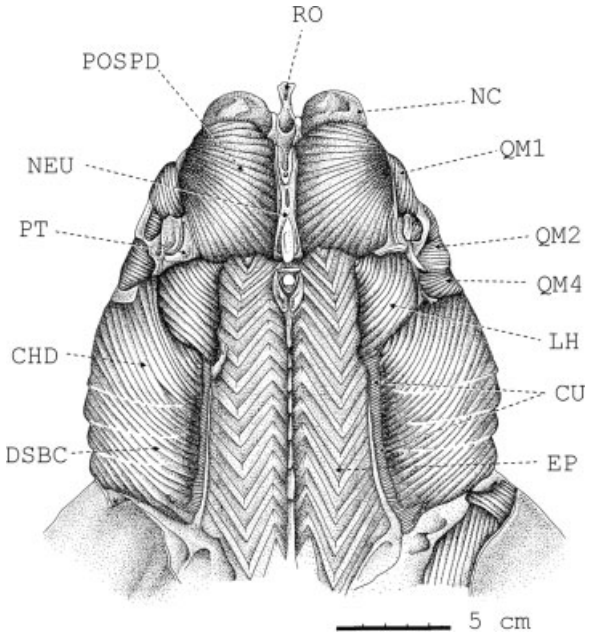

Fig. 2. Dorsal view of the head of a 97 cm TL male *Ginglymostoma cirratum* with the skin removed and muscle fiber direction indicated. Myosepta of the epaxialis are indicated without fiber direction. CHD, constrictor hyoideus dorsalis; CU, cucullaris; DSBC, dorsal superficial branchial constrictor; EP, epaxialis; LH, levator hyomandibularis; NC, nasal capsule; NEU, neurocranium; POSPD, superficial head of posterior division of preorbitalis; PT, postorbital process; QM1, quadratomandibularis division 1; QM2, quadratomandibularis division 2; QM4, quadratomandibularis division 4; RO, rostral cartilage. (Reproduced from Motta and Wilga, J Morphol, 1999, 249, 1–29, © Wiley-Liss, a subsidiary of John Wiley and Sons).

end of the ceratohyal every 4 mm with a 3 mm table, 3 second exposure, and 280 milliamps at 125 kv. A CAMRA® software program, version 5.0.1 (ISG Technologies, Ontario, Canada), was used to reconstruct the images to produce three-dimensional images of the head.

Electromyography

Six juvenile (64–98 cm TL, five male and one female) *Ginglymostoma cirratum* were maintained in a 5 m diameter holding tank, provided with filtered, flow-through seawater, at Mote Marine Laboratory, Sarasota, Florida. Approximately 4 weeks prior to electromyography (EMG) experiments, the sharks were transferred to a 2.4 m diameter, 1400 L semicircular experimental tank with an acrylic window for a training period. Water temperature ranged from 26 to 29°C. Sharks were fed cut pieces of Atlantic thread herring (*Opisthonema oglinum*) and crevalle jack (*Caranx hippos*) three times per week. Food size was approximately half the diameter of the shark's mouth. Food was placed on the floor of the tank, on a clear acrylic platform or gently held in wooden tongs and released just prior to suction capture. In most cases the shark remained stationary and propped itself on its pectoral fins as it took the food. In all experiments sharks were fed to satiation, which ranged from 11 to 44 pieces of food per shark.

After the training period, sharks were prepared for EMG experiments. The EMG experiment protocol follows that of Motta et al. (1997). Sharks were anesthetized with 0.133 g l^{-1} MS-222 (tricaine methanesulphonate) in a recirculating seawater/anesthetic ventilation system. Bipolar electrodes (0.06 mm diameter) with 1 mm at the ends stripped of insulation were implanted in the cranial musculature with 23-gauge hypodermic needles according to a stereotactic map of the head (Motta and Wilga, 1999). Electrodes were implanted in the following cranial muscles: epaxialis (EP), superficial head of the posterior division of the preorbitalis (POSPD), anterior division of the preorbitalis (POAD), quadratomandibularis divisions 1–4 (QM), levator hyomandibularis (LH), coracoarcualis (CC), coracohyoideus (CH), coracobranchialis (CB), coracomandibularis (CM), interhyoideus (IH), and levator palatoquadrati (LP) (Figs. 1–4) (Motta and Wilga, 1999). Each electrode wire was secured to the skin of the shark using cyanoacrylate glue and then all wires were glued together using polystyrene cement and attached to a loop of suture through the dorsal fin. These wires (~2 m length) were connected via a 3-m cable to differential amplifiers (AM Systems, Sequim, WA) (gain 1,000X, band-pass filter 100–3,000 Hz, 60 Hz notch filtered). Implantation of the leads took ~45 min, and after recovering from anesthesia (5–10 min) the shark was allowed to rest for ~1 h before feeding commenced. Of the 14 muscles, generally six or seven muscles were simultaneously monitored per shark per experiment, although in most cases fewer muscles produced usable motor activity due to a variety of implantation or recording problems. Signals were simultaneously recorded on a Mark-11 thermal array recorder (Western Graphtec, Santa Ana, CA) and on VHS tape through a pulse-code modulator (model 3000A, A.R. Vetter, Rebersburg, PA). At the termination of the experiment, the shark was euthanatized with a 0.5 g l^{-1} overdose of MS 222 in order to surgically verify the position of the implanted electrodes.

Analog EMG data were digitized by an analog-to-digital converter at a sample rate of 8,333 Hz, and analyzed by a custom EMG analysis program in Spike 2 software (model 1401 plus, Cambridge Electronics Design, Cambridge, UK). Motor patterns of 127 suction captures from the six sharks were analyzed for burst duration, sequence, and timing relative to the onset of the coracomandibularis, the primary lower jaw depressor. Only suc-

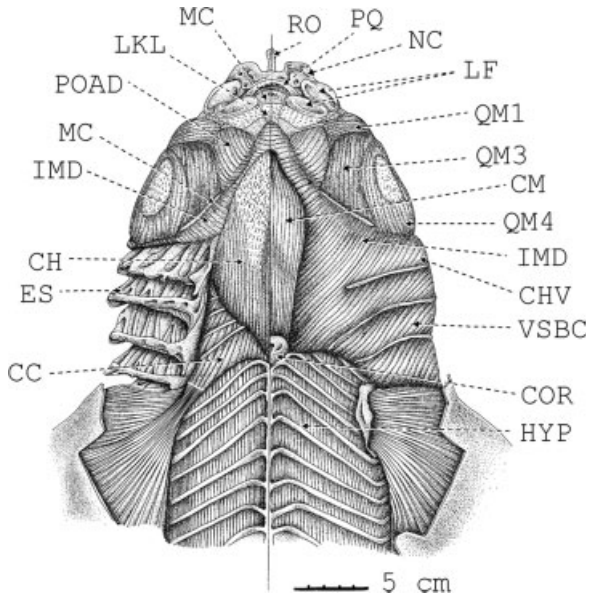

Fig. 3. Ventral view of the head of a 97 cm TL male *Ginglymostoma cirratum* with the skin removed and muscle fiber direction indicated. The intermandibularis and ventral superficial branchial constrictor are cut on both sides to expose deeper muscles. The coracomandibularis is removed on the right side exposing the deeper coracohyoideus. Branchial constrictors are removed on the right side to expose the cartilaginous extra-septalia. CC, coracoarcualis; CH, coracohyoideus; CHV, constrictor hyoideus ventralis; CM, coracomandibularis; COR, coracoid; ES, extra-septalia; HYP, hypaxialis; IMD, intermandibularis; LF, labial folds; LKL, knob-labium ligament; MC, mandibular cartilage; NC, nasal capsule; POAD, anterior division of preorbitalis; PQ, palatoquadrate; QM1, quadratomandibularis division 1; QM3, quadratomandibularis division 3; QM4, quadratomandibularis division 4; RO, rostral cartilage; VSBC, ventral superficial branchial constrictor. (Reproduced from Motta and Wilga, J Morphol, 1999, 249, 1–29, © Wiley-Liss, a subsidiary of John Wiley and Sons).

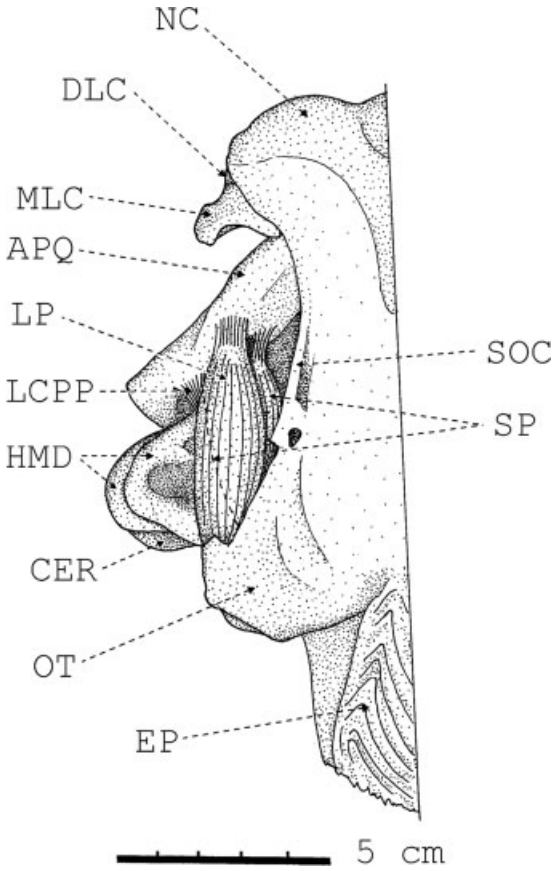

Fig. 4. Deep dorsal view of the left chondrocranium, mandibular and hyoid arch of a 123 cm TL male *Ginglymostoma cirratum*. The orbit and postorbital process are removed to expose the levator palatoquadrati and spiracularis muscles. APQ, ascending process of palatoquadrate; CER, ceratohyal; DLC, dorsal labial cartilage; EP, epaxialis; HMD, hyomandibula; LCPP, chondrocraniopalatoquadrate ligament; LP, levator palatoquadrati; MLC, medial labial cartilage; NC, nasal capsule; OT, otic capsule; SOC, supraorbital crest; SP, spiracularis. (Reproduced from Motta and Wilga, J Morphol, 1999, 249, 1–29, © Wiley-Liss, a subsidiary of John Wiley and Sons).

tion capture bites were analyzed in this manner as the food item was generally sucked directly into the buccopharyngeal cavity in one suction event. Manipulation bites, during which the shark crushes the food, were not analyzed.

Kinematics

Video recordings of 29 prey capture events were taken on a total of seven *Ginglymostoma cirratum* in which the sharks were lateral to the camera and the food was not restrained by tongs at the start of capture. Filming was performed on two sharks (79 and 80 cm TL) from the above EMG experiments and five other sharks (61–103 cm TL) from the study of Matott et al. (2005), with food presented in a similar manner. The first two sharks were recorded with a NAC HSV-200 (Tokyo, Japan) video camera at 200 fps. Video of the captures was downloaded to computer with a Panasonic AG-1970 (Osaka, Japan) video analyzer and distances measured with Sigma Scan Pro 4 software (SYSTAT Software, Point Richmond, CA). Because video recording was not synchronized to electromyography in these experiments, simultaneous analysis of kinematic and motor activity was not possible. The five additional *G. cirratum* (61–103 cm TL) were fed pieces of Atlantic thread herring (*Opisthonema oglinum*) or squid (*Loligo* sp.) cut in length equal to approximately one or two times the mouth diameter of the shark. Images were recorded with a Redlake PCI 1000 (Redlake MASD, Tucson, AZ) digital video camera at 250 fps. For the latter experiment, water temperature varied from 22–27°C (Matott et al., 2005). For all captures, the following measurements were taken with Motionscope 2.30 software (Redlake MASD, San Diego, CA) beginning with the field when the food began to move towards the mouth: 1) distance from the food to the anterior margin of the mandible; and 2) velocity of mandible depression (distance traveled by tip of mandible/duration of mandible depression). As in other studies of *G. cirratum* and *Chiloscyllium plagiosum*, maximum hyoid depression could not be accurately determined because of the ventral bulging of the buccopharyngeal cavity due to water inflow (Motta et al., 2002; Matott et al., 2005; Wilga et al., 2007). Consequently, in these studies the timing of mandible depression is used as a proxy for buccopharyngeal expansion.

The distance moved by the food until it reached the anterior margin of the mandible was linearly regressed against total length and against the velocity of mandible depression for all food sizes combined, and separately for mouth-width sized food (the majority of captures). An ANOVA was then performed on the regressions. In addition, for 28 of the captures, the distance of the food above the substrate was measured just prior to it entering the mouth. This height was tabulated as either less

than or greater than one mouth-width above the substrate as the proximity to the substrate is known to affect suction distance (Nauwelaerts et al., 2006). The absolute distance (cm) food was sucked into the mouth was then compared for the two heights. Small sample size precluded statistical analysis.

Suction Measurements

In vivo suction pressure at the mouth opening was recorded from 14 semicaptive *Ginglymostoma cirratum* from two locations. The first group of five sharks was entrained in a large canal (~50 m wide) in Port St. Lucie, Florida at 23°C. These sexually mature sharks (3 males, 2 females) ranged in size from 153–206 cm TL. Suction pressure was also measured in nine semicaptive sharks (135–224 cm TL, male and female both present but number of each not recorded) in a shallow (1 m deep by 3 m wide) lagoon at the Keys Marine Laboratory, Long Key, Florida. Water temperature was not recorded. Video images were not recorded for either group.

Because of the large size of the holding facilities and sharks pressure transducers could not be implanted in these freely swimming animals. Consequently, pressures were recorded by transducers mounted in PVC feeding tubes. A Mikro-Tip® pressure transducer (MPC-500) and TCB-500 Transducer Control Unit (Millar Instruments Corp., Houston, TX) were connected to one channel of a Yokogawa DL-716 (Tokyo, Japan) digital oscilloscope. The ~1 mm diameter pressure transducer was housed in a 1.6 cm internal diameter PVC pipe so that the distal end of the transducer was positioned parallel to the water flow 1–2 mm from the opening of the pipe. A rubber plug 1 cm within the pipe, with a 1 mm diameter hole for the transducer, was sealed with silicone glue to prevent water flow around the plug. Pieces of squid mantle (*Loligo* sp.), and skin with attached muscle from various bony fishes (*Sphyraena barracuda*, *Anisotremus surinamensis*, *Caranx hippos*) were wrapped around the pipe and held in place with rubber bands. Mouth width which ranged from 8 to 12 cm, greatly exceeded the diameter of the pipe and attached food, therefore obstruction of the mouth during suction was minimized. However, obstruction of the mouth aperture by the pipe and food may have resulted in slightly greater subambient pressures (but see Discussion).

The pipe with transducer was submerged approximately 0.3–0.5 m into the water and offered to a shark. Only suction captures in which the shark placed its mouth around or very near to the pipe and food and then sucked the food off were recorded. For cases in which the shark repeatedly sucked the apparatus before dislodging the food, each suction attempt was recorded as long as the subambient pressure returned to ambient between suctions. A total of 58 suction captures from 14 sharks were recorded. At the termination of the experiment, the transducer was calibrated by connecting it to an OMEGA® manual PGT temperature-compensated pressure gauge (Omega Engineering, Stamford, CT) and a vacuum pump. The voltage output from the pressure transducer was recorded with pressures from 0 to −96 kPa, and a linear regression ($n = 16$, $r^2 = 0.99$) of voltage against pressure was used to correct any slight error of the Millar instruments. The Millar transducers have a factory specified error of ±0.5%.

For the 58 suction captures, the duration from the onset of pressure decline to the peak subambient pressure (in ms) and the peak subambient pressure (in kPa) were measured using LabVIEW 6.0 software (National Instruments Corp., Austin, TX). The reported subambient pressure is the maximum subambient suction pressure generated minus the ambient pressure at depth just prior to suction initiation. Duration to peak subambient pressure was linearly regressed against the peak subambient pressure and an ANOVA was performed on the regression. In addition, the single greatest suction pressure for each shark ($n = 14$) was linearly regressed against total length, and an ANOVA was performed on the regression to determine if a significant relationship existed between the two.

To compare subambient pressure within the buccopharyngeal cavity (termed hyoid pressure) and at the entrance to the cavity (termed buccal pressure), three additional *Ginglymostoma cirratum* (82 cm TL male, 83 cm TL female, 103 cm TL male) maintained at 24°C at Mote Marine Laboratory were anesthetized as in the electromyography experiments and implanted with a SPR-249 pressure transducer within a plastic catheter (Millar Instruments Corp., Houston, TX). To measure the hyoid pressure, the buccopharyngeal cavity was fitted with a catheter through the first gill slit and sutured to the center of the oral cavity roof just anterior to the first gill slit above the basihyal, with the tip of the transducer protruding from the catheter parallel to the water flow. The external end of the catheter was sealed with silicone glue to prevent reverse water flow through it. The transducer was connected to a TCB-500 transducer control unit. An external MPC-500 pressure transducer housed in a PVC pipe was wrapped with squid and fish (as abovementioned) and presented to the shark such that simultaneous hyoid and buccal pressures were recorded for 46 suction captures. Once the transducers were at the appropriate depth and temperature acclimated, the control unit was recalibrated to remove the slight increase in subambient pressure with depth. Data were acquired with a 6020E National Instruments data acquisition board and LabVIEW 6.0 software. The SPR-249 pressure transducer was calibrated as earlier ($n = 15$, $r^2 = 0.99$).

Simultaneous video images of the suction captures were recorded with dual Redlake PCI-1000 and PCI-500 digital video cameras at 250 fps and synchronized to the pressure profiles by means of a digital electronic pulse signal. Only suction events in which the external PVC pipe and transducer were at the anterior end of the oral aperture at the time of suction were used. In most cases the shark's mouth enclosed the tip of the PVC pipe. Using LabVIEW 6.0 and Motionscope 2.30 software (Redlake MASD, San Diego, CA) the duration and timing of mandible depression, in addition to peak hyoid and buccal pressure and timings, were calculated. For these capture events the peak hyoid and buccal pressures were linearly regressed against the duration from onset to peak hyoid and buccal pressures, respectively, as well as the duration of mandible depression. ANOVA was performed on each. Peak hyoid and buccal pressures were compared by a *t*-test after natural log transformation. All the aforementioned ANOVA, linear regressions and *t*-tests, as well as Kolmogorov-Smirnov and Levene Median tests for normality and equality of variance, were performed with Sigma-Stat 2.03 (SYSTAT Software, Point Richmond, CA).

RESULTS

Anatomy

Manipulation of the intact head of *Ginglymostoma cirratum* indicates that when the mandible and hyoid arch are depressed and the palatoquadrate cartilage protruded, the distal end of the ceratohyal moves posteroventrally, pivoting on its articulation with the distal hyomandibula (Fig. 5A–F). The basihyal concomitantly moves posteroventrally, depressing the floor of the buccopharyngeal chamber (Fig. 5C,D,G,H). The hyomandibula pivots on the cranium such that its distal end moves ventrally (Fig. 5C–F). The diarthrosis between the distal hyomandibula and mandible moves ventrally as the mouth is opened, and the ceratohyal loses its abutment against the mandible (Fig. 5C,D,G,H). As the ceratohyal-basihyal complex moves posteroventrally, it greatly expands the floor of the buccopharyngeal cavity ventrally because of the loose ligamentous connection

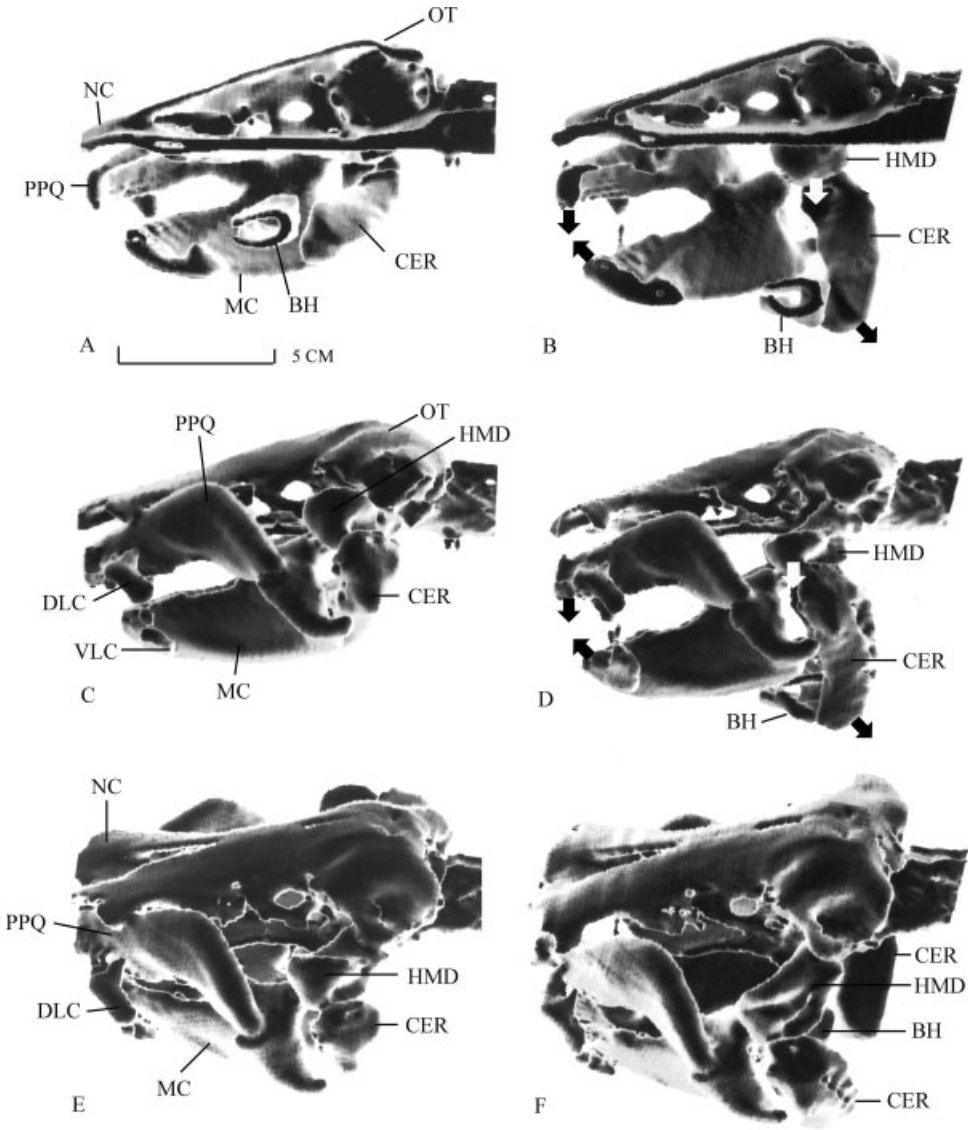

Fig. 5. The chondrocranium, mandibular, and hyoid arches of two intact *Ginglymostoma cirratum* heads reconstructed through Computer Axial Tomography. Left figures with jaw closed are from a male 57 cm TL shark. Right figures from a 123 cm TL male indicate position of the elements during jaw protrusion and adduction, with mandible manually depressed, labial cartilages extended and palatoquadrate protruded. Large arrows in B and D indicate direction of movement of select skeletal elements. **A,B**: Mid-sagittal view showing position of the ceratohyal and basihyal relative to the jaws. Note that the basihyal is retracted posteroventrally during jaw opening. **C,D**: Left lateral view indicating position of the hyomandibula, ceratohyal, and basihyal. The labial cartilages swing anteriorly to laterally occlude the mouth. A loose association between the ceratohyal and mandible results in large ventral expansion of the buccopharyngeal cavity despite mouth size limitation by the labial cartilages and ligaments. **E,F**: Dorsolateral view showing position of the hyomandibula and its change of angle during jaw opening. **G,H**: Ventral view indicating the relative position of the basihyal and ceratohyal when the mouth is open. **I,J**: Dorsal view indicating position of the hyomandibula and ceratohyal APQ, ascending process of palatoquadrate; BH, basihyal; CER, ceratohyal; DLC, dorsal labial cartilage; HMD, hyomandibula; MC, mandibular cartilage; MLC, medial labial cartilage; NC, nasal capsule; OT, otic capsule; PPQ, palatine process of palatoquadrate; PQ, palatoquadrate; SUST, sustentaculum; VLC, ventral labial cartilage.

between the mandible and hyoid arch (Motta and Wilga, 1999). The mandibulohyoid connective tissue sheath that forms the floor of the buccopharyngeal cavity and attaches to the ceratohyals, basihyal, mandible anteriorly, and the branchial arches posteriorly (Motta and Wilga, 1999), moves ventrally. The labial cartilages move anteriorly to laterally bound the mouth, forming a roughly circular mouth orifice.

Motor Activity

Mandible depression is initiated by activity of the coracomandibularis (CM), which precedes ac-

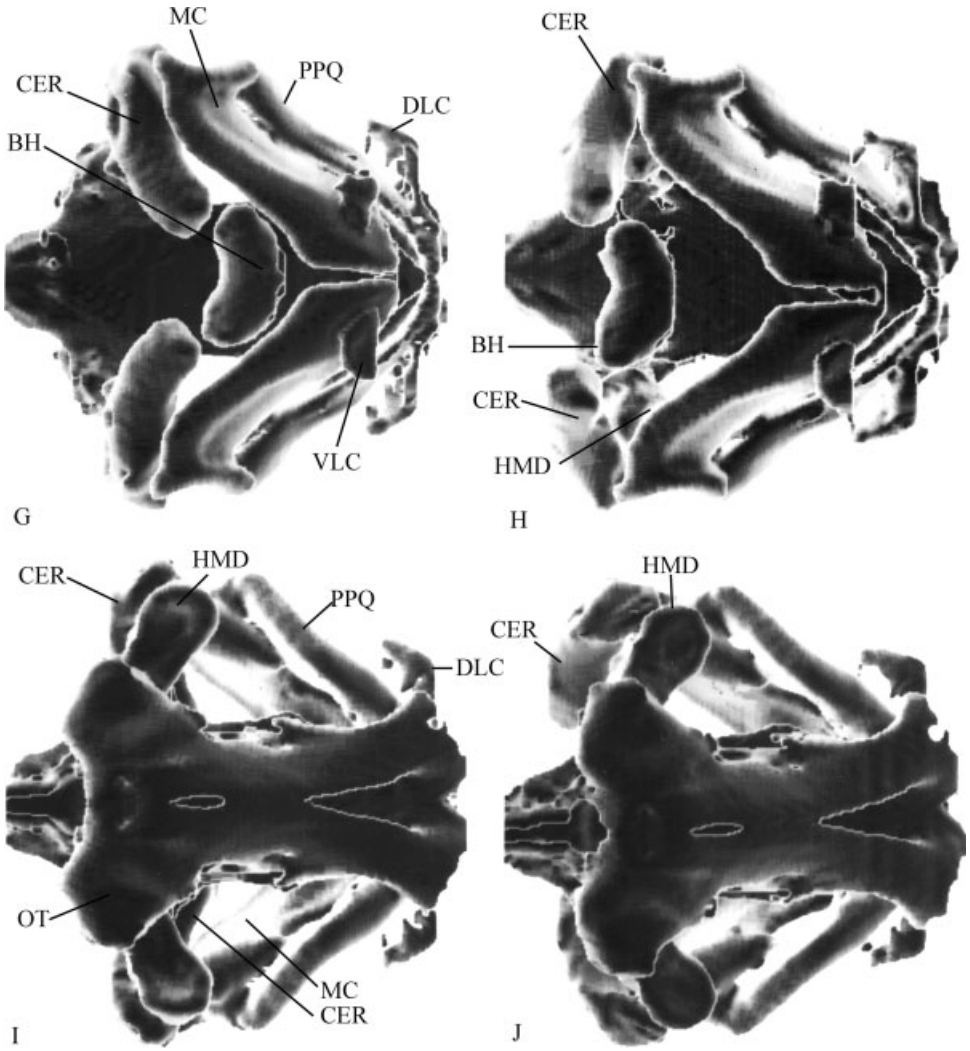

Fig. 5. (Continued.)

tivity of all other muscles (see Fig. 6). Stabilization or elevation of the cranium is then effected by the epaxialis (EP). Hyoid and branchial depression follow due to firing of the coracohyoideus, coracobranchiales, and coracoarcualis (CH, CB, CC). Temporally this abduction is led by activity in the coracohyoideus, which inserts on the basihyal and ceratohyals. Mandibular adduction resulting from interhyoideus (IH) muscle activity overlaps jaw adduction by the quadratomandibularis (QM) complex and the preorbitalis complex (POAD, POSPD). Following this, the levator palatoquadrati (LP) and the levator hyomandibuli (LH) retract the palatoquadrate and hyomandibular cartilages.

Suction Performance

In every case food was captured by suction. The food was either sucked into the buccopharyngeal cavity directly, or sucked towards the mouth and then grasped by the teeth. In the latter case, the food was generally transported farther into the buccopharyngeal cavity with subsequent suctions. On occasion larger food items were torn apart by repeatedly being spit out and sucked back into the mouth. The greatest suction subambient pressure recorded at or near the mouth aperture was −110 kPa. There was no significant relationship between peak subambient pressure and shark total length (d.f. = 1,12 $F = 0.314$, $P = 0.586$) (Fig. 7A). The mean peak subambient pressure for the 14 semicaptive sharks was −46 kPa (SE = ±2.9 kPa) and was reached in approximately 64 ms (SE = ±4.7 ms). The time-to-peak subambient pressure was negatively related to peak subambient pressure, indicating that greater subambient pressures are achieved by the rapid generation of suction pressure (Fig. 7B) (d.f. = 1, 56 $F = 14.203$, $P < 0.001$). Pressure profiles varied from relatively weak suction captures that were protracted in duration to very rapid events with large drops in pressure (see Fig. 8).

Simultaneous recordings of hyoid and buccal pressures indicate that hyoid pressure starts to

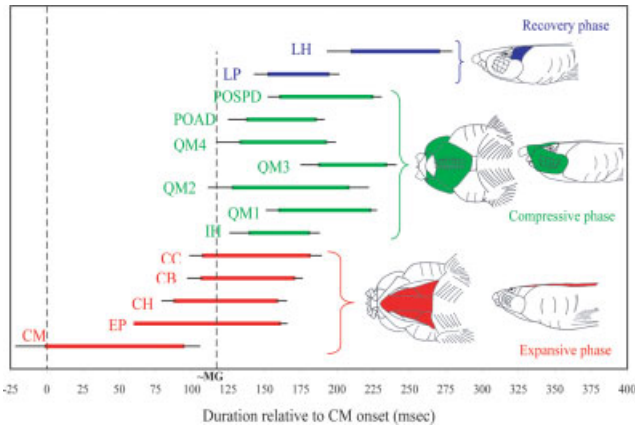

Fig. 6. Composite electromyographic profile of *Ginglymostoma cirratum* suction food capture with durations scaled to the onset of coracomandibularis activity. Heavy colored lines indicate duration of muscle activity, error bars on the left indicate one standard error of the onset relative to the onset of EP (the most consistently firing muscle), and error bars on the right are one standard error for duration of motor activity for each muscle. Subsequent bursts of activity that occur for some muscles are not illustrated. The approximate time of maximum gape/mouth opening (Baumgartner, 1992) based on Matott et al. (2005) is indicated. Red indicates muscles active during the expansive phase, green the compressive phase, and blue the recovery phase. Line drawing at right is from a 172 cm TL shark with the jaws and hyoid arch manually manipulated into the approximate position based on video images. The expansive illustration phase shows the mouth at maximum expansion, the labial cartilages anteriorly flared, and expansive phase muscles in red. See Figures 1–4 for muscle nomenclature. The compressive phase illustrates the hyoid maximally depressed, the hyomandibula anteroventrally depressed and the mandible adducted against the maximally protruded upper jaw. The labial cartilages are removed to visualize the protruded upper jaw, and active muscles are green. The recovery phase is illustrated with the mouth closed and upper jaw retracted, hyoid and hyomandibula elevated, and labial cartilages retracted into the resting position. The levator palatoquadrati muscle is deep to the blue levator hyomandibuli and the eye and is not visible. CB, coracobranchiales; CC, coracoarcualis; CH, coracohyoideus; CM, coracomandibularis; EP, epaxialis; IH, interhyoideus; LH, levator hyomandibuli; LP, levator palatoquadrati; POAD, anterior division of preorbitalis; POSPD, superficial head of posterior division of preorbitalis; QM1, quadratomandibularis division 1, QM2, quadratomandibularis division 2, QM3, quadratomandibularis division 3, QM4, quadratomandibularis division 4.

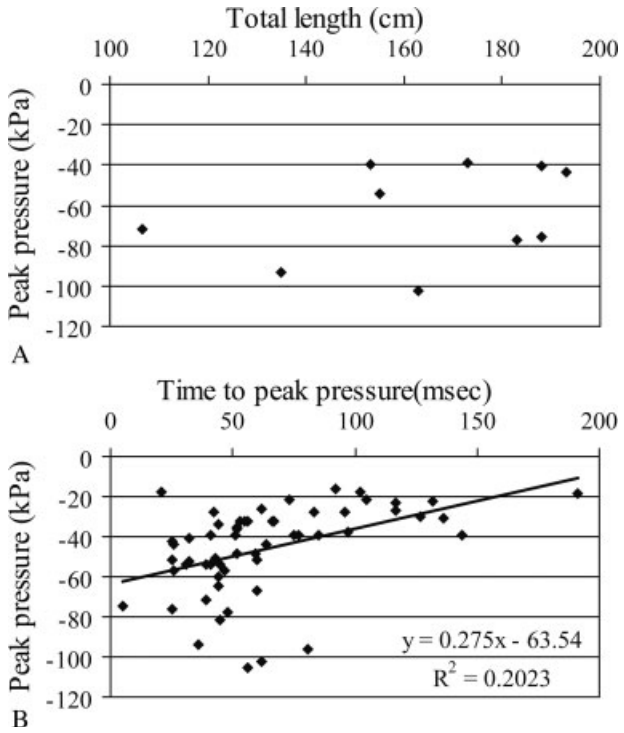

Fig. 7. **A**: The single greatest peak subambient suction pressure recorded for each of 14 sharks plotted against their respective total length. ANOVA revealed no relationship between the two variables. **B**: Linear regression of peak subambient pressure against the time to reach peak pressure from the start of pressure drop for 58 suction captures from 14 *Ginglymostoma cirratum*. To normalize data log-transformed values are used for the linear regression and ANOVA, but absolute values are expressed on a log scale for clarity, with pressures expressed as negative values in keeping with the increase of subambient pressure. The shorter the duration taken to reach the peak subambient pressure (during each suction event), the greater the negative pressure.

drop approximately 27 ms (SE = ±4 ms) prior to buccal pressure at the oral aperture (see Fig. 9). Peak hyoid pressure occurred 14 ms (SE = ±3 ms) before peak buccal pressure. Average hyoid and buccal pressures were 16.0 and 24.9 kPa (SE = ±1.8, 2.4), respectively, and differed significantly (d.f. = 90, t = 3.494, $P < 0.001$). Hyoid pressure starts to decline 31 ms (SE = ±4 ms), and buccal pressure 5 ms (SE = ±4 ms), before the start of mandible depression. Therefore, peak hyoid pressure occurred 1 ms before (SE = ±3 ms), and peak buccal pressure 13 ms (SE = ±3 ms), after peak mandible depression. As in the semicaptive sharks (64 ms), the duration to peak buccal pressure was 58 ms (SE = ±4 ms) from the start of the buccal pressure decline until the peak pressure. The duration to peak hyoid pressure was 70 ms (SE = ±5 ms) from the start of hyoid pressure decline until peak pressure. Maximum gape occurs 1 ms after peak mandible depression. There was no relationship between peak hyoid and buccal pressure and the time-to-peak subambient pressure (d.f. = 1.51, F = 0.599, P = 0.442; d.f. = 1.51, F = 1.115, P = 0.296, respectively), and no relationship between peak hyoid or buccal pressure and duration of mandible depression (d.f. = 1.48, F = 0.002, P = 0.962; d.f. = 1.48, F = 0.0321, P = 0.859, respectively).

Food was sucked into the mouth from a maximum distance of 3.0 cm or 51% of mouth width (n = 7 sharks, 29 captures) from the anterior margin of the mandible, averaging 1.2 cm (SE = ±0.1 cm), approximately 24% of mouth-width. There was no relationship between suction distance and shark total length for all food sizes combined (d.f. = 1, F = 1.551, P = 0.224) or only smaller food items (d.f. = 1, F = 1.665, P = 0.214), nor any relationship

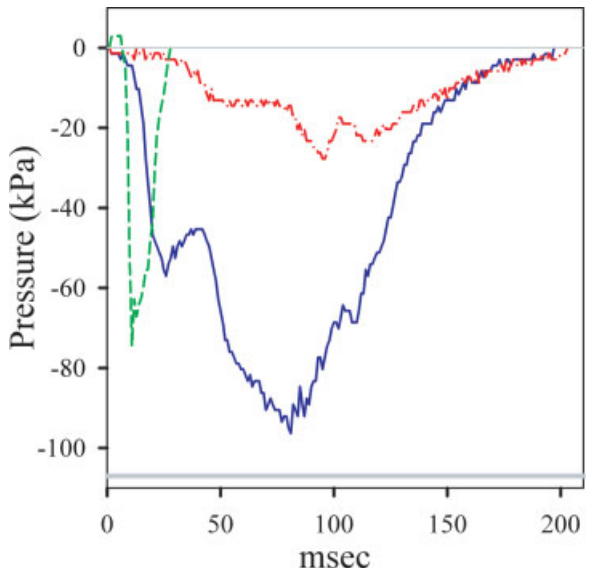

Fig. 8. Three representative buccal pressure profiles from different semi-captive adult *Ginglymostoma cirratum* demonstrating the variability in suction performance during feeding. Some captures are extremely rapid with large subambient pressures (green dashed line), others can approach −1 atmosphere but be more prolonged (blue solid line), whereas others may generate little subambient pressure (red dash-dot line). The lower gray line indicates −1 atmosphere pressure at the average depth of the probe (~0.5 m).

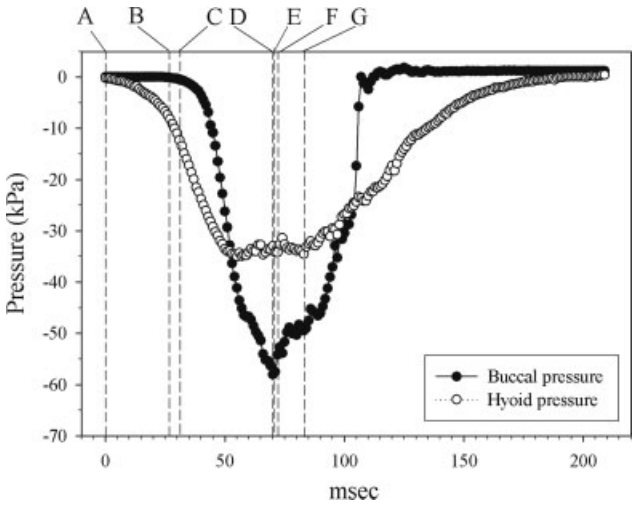

Fig. 9. Representative pressure profile for a 103 cm TL male *Ginglymostoma cirratum* indicating simultaneous hyoid and buccal pressures. Dotted lines indicate average value for 46 suction captures from three sharks superimposed on a representative profile. Average buccal pressure is 9 kPa greater than hyoid pressure. Note that the onset of hyoid pressure drop (time zero) (**A**) precedes the onset of the buccal pressure drop (**B**) by 27 ms, the hyoid pressure decline precedes the start of mandible depression (**C**) by 31 ms, peak hyoid pressure (**D**) occurs 70 ms from time zero, followed 1 ms later by peak mandible depression (**E**), then another 1 ms later by maximum mouth opening (**F**). Peak buccal pressure (**G**) occurs 84 ms after time zero.

between suction distance and mandible depression velocity for all food sizes combined (d.f. = 1, F = 2.223, P = 0.148) or smaller items only (d.f. = 1, F = 0.188, P = 0.670). There was no apparent difference in the distance that food was sucked in based on the height of the food (or shark's mouth) above the floor of the tank; however, small sample size precluded statistical analysis. When food was less than one mouth-width above the substrate the mean suction distance was 1.0 cm (±0.1 SE), and for distances greater than one mouth-width the suction distance was 1.5 cm (±0.2 SE) for food of one and two mouth-width sizes combined. When only mouth-width size food was considered, the suction distances were 1.0 cm (±0.1 SE) and 1.2 cm (±0.1 SE), respectively.

DISCUSSION

Cranial Mechanics

Suction generation in *Ginglymostoma cirratum* occurs by buccopharyngeal expansion mediated by jaw abduction and hyoid and branchial arch depression during the expansive phase of the gape cycle. As in bony fishes (Lauder, 1985; Sanford and Wainwright, 2002; Westneat, 2006), suction feeding in *G. cirratum* is characterized by expansive, compressive, and recovery phases, but differs in that the preparatory phase may be lacking (Wu, 1994; Motta et al., 2002; Matott et al., 2005). During the expansive phase, lower jaw depression effected by the coracomandibularis muscle preceded all other kinematic and motor activities (Motta et al., 2002) (see Fig. 6). Depression of the hyoid (basihyal and ceratohyal) and expansion of the branchial arches are driven by contraction of the rectus cervicis group (coracoarcualis and coracohyoideus) and the coracobranchiales. This is similar to the situation in other sharks (Motta et al., 1997; Wilga and Motta, 2000).

The following evidence supports the idea that suction generation is primarily linked to hyoid and branchial depression and less to mandible depression in *Ginglymostoma cirratum*. The hyoid pressure started to drop 27 ms prior to buccal pressure and 31 ms prior to the start of mouth opening. There also was no relationship of peak buccal or hyoid pressure and the duration of mandible depression. Contraction of the rectus cervicis muscle group continued after maximum mouth opening, and the coracomandibularis muscle activity ceased before or just after maximum opening was attained, indicating continued depression of the floor of the mouth and pharyngeal cavity after mandible depression ceases (Matott et al., 2005) (see Fig. 6). However, lacking simultaneous recording of branchial and hyoid movement together with pressure we cannot conclusively demonstrate this.

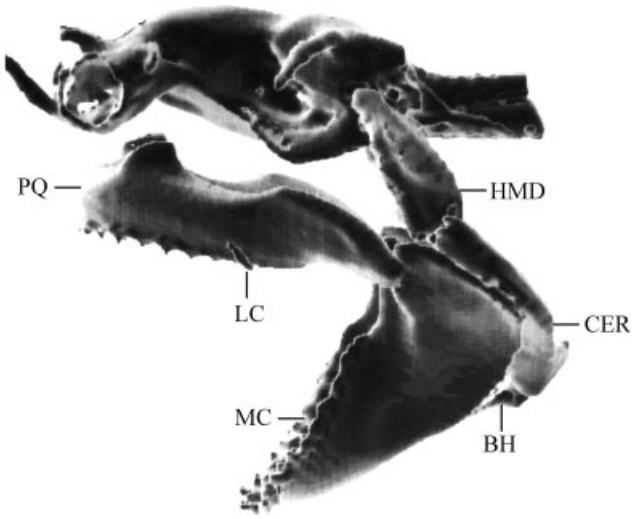

Fig. 10. The chondrocranium, mandibular, and hyoid arches of an intact 150 cm TL *Negaprion brevirostris* head reconstructed through Computer Axial Tomography with mandible manually depressed, and palatoquadrate maximally protruded. A tight association between the ceratohyal and mandible results in a coupling such that the buccopharyngeal cavity cannot be depressed to the extent of *Ginglymostoma cirratum* (Fig. 5D). The relatively small labial cartilages (only partly visible due to their small size) do not limit mouth size. BH, basihyal; CER, ceratohyal; HMD, hyomandibula; LC, labial cartilage; MC, mandibular cartilage; PQ, palatoquadrate (Reproduced from Motta and Wilga, J Morphol, 1995, 226, 309–329, ©Wiley-Liss, a subsidiary of John Wiley and Sons).

The nurse shark's prey capture mechanics can be likened to the expansion of a bellows. Contraction of the coracobranchiales, coracoarcualis, and coracohyoideus depresses the entire floor of the buccopharyngeal cavity because of the attachment of the branchial arches, ceratohyals, and basihyal to the mandibulohyoid connective tissue sheath that forms the floor of this cavity (Motta and Wilga, 1999). Radiography and manipulation revealed that the ceratohyals and basihyal can pivot substantially on the hyomandibula, greatly depressing the floor of the bucopharyngeal cavity below the depressed mandible for voluminous buccopharyngeal expansion (see Fig. 5). This is quite different than the case in carcharhinid sharks where tighter ligamentous coupling between the ceratohyal and mandible limits depression of the floor of the buccopharyngeal cavity even though the vertical mouth height is large (see Fig. 10). *Ginglymostoma cirratum* mouth size, both horizontal and vertical, is small and tightly bound by large labial cartilages and ligaments restricting its size for high velocity suction feeding, but the loose connection between the ceratohyal and mandible permits substantial ventral buccopharyngeal depression (Figs. 5D and 10; see also Fig. 5 in Motta and Wilga (1995) and Fig. 2 in Motta and Wilga (1999)).

Although a kinematic analysis only revealed measurable cranial elevation in 15% of suction captures (Motta et al., 2002), there was some activity of the epaxialis muscles during most suction captures (Matott et al., 2005). This muscle may serve as an antagonist to the mandible and hyoid depressors, holding the head level during the strike. In approximately 35% of *Ginglymostoma cirratum* strikes the head depresses rather than elevates (Motta et al., 2002; Matott et al., 2005). *Chiloscyllium plagiosum* also exhibits minimal cranial elevation even when capturing large food or elusive benthic prey (Lowry and Motta, 2007a). Lack of cranial elevation in *G. cirratum* might be related to the terminal position of the mouth, such that the cranium need not be elevated to align a subterminal mouth with prey directly in front of the predator, as occurs in many carcharhinid and lamnid sharks (Motta et al., 2002).

During the compressive phase muscle activity by the interhyoideus and the intermandibularis indicates that the hyoid and mandible of *Ginglymostoma cirratum* were adducted respectively, and the quadratomandibularis complex adducted the jaws (see also Matott et al., 2005). The preorbitalis muscles were active during the end of the compressive phase (see Fig. 6). In *Chiloscyllium plagiosum* jaw closure during suction capture is entirely due to upper jaw protrusion powered by the quadratomandibularis with the preorbitalis aiding in hyoid elevation during the recovery period. However, during biting the preorbitalis aids in jaw closure, contributing to a more forceful bite (Ramsay and Wilga, 2008). Upper jaw protrusion in *G. cirratum* starts in the expansive phase and peaks at the end of the compressive phase as lower jaw elevation ceases (Motta et al., 2002). Lacking simultaneous electromyography, video, and positional data of the cartilaginous elements, we are not able to ascertain the mechanism of upper jaw protrusion. Muscle activity during what appears to be the recovery phase, in which the cartilaginous elements are returned to their starting positions, overlapped the end of the compressive phase and included activity in the levator palatoquadrati and the levator hyomandibulae. The levator palatoquadrati lies almost horizontally in *G. cirratum*, originating on the otic capsule and inserting on the palatoquadrate cartilage (Fig. 4; Motta and Wilga, 1999). The only possible action of the levator palatoquadrati is to retract the palatoquadrate cartilage posteriorly and, together with the levator hyomandibuli, retract the entire jaw apparatus and hyoid as they are bound together by ligaments (Motta and Wilga, 1999).

Comparison to Bony Fish Suction Mechanics

The kinematics and mechanical couplings involved with suction feeding in *Ginglymostoma*

cirratum differ from those of bony fishes in many respects, yet the functional outcome is similar. In bony fishes the generation of suction pressures that entrain food in a flow of water into the mouth result from buccal expansion, which is a consequence of rapid cranial elevation, suspensorial abduction, mandible depression, upper jaw protrusion, and hyoid depression (Osse, 1969; Lauder, 1985; Gibb and Ferry-Graham, 2005; Westneat, 2006). Unlike bony fishes, cranial elevation in sharks apparently plays little or no role in buccal expansion for suction feeding (Edmonds et al., 2001; Motta et al., 2002; Matott et al., 2005; Huber et al., 2006; Lowry and Motta, 2007a). Perhaps this is because cranial elevation in bony fishes is mechanically coupled to upper jaw protrusion, providing dorsal expansion in addition to lateral and ventral expansion of the buccal cavity (Westneat, 1990). In sharks, upper jaw protrusion is neither linked to cranial elevation—it may occur during either the expansive or compressive phase—nor does it increase buccal volume to any appreciable extent (Wu, 1994; Motta et al., 1997; Wilga and Lauder, 2001).

While the lack of a rigid operculum in sharks most likely precludes generation of large subambient pressures in the parabranchial chamber, depression of the hyoid and branchial cartilages generates suction, similar to that in bony fishes. During respiration in the swellshark *Cephaloscyllium ventriosum*, small subambient pressures are recorded in the parabranchial chamber (Ferry-Graham, 1999). This parabranchial subambient pressure may result from branchial arches that are not able to completely occlude the buccopharyngeal and parabranchial chambers during pressure decline in the former chamber.

During the expansive phase buccopharyngeal expansion in *Ginglymostoma cirratum* proceeds in an anterior to posterior direction, resulting in the capture and transport of the food, and eventual flushing of the entrained water out of the pharyngeal slits (Motta et al., 2002). The anterior swinging of the large labial cartilages in many suction feeding sharks, including *G. cirratum*, laterally occludes the mouth in a manner analogous to the maxillae in bony fishes, resulting in an anteriorly directed, relatively small oral aperture. This increases the effectiveness of suction feeding because, for a given rate of volumetric buccopharyngeal expansion, flow velocity into the mouth is inversely proportional to the size of the mouth aperture (Lauder, 1979; Day et al., 2005; Wainwright and Day, 2007). Lastly, suction feeding in both sharks and bony fishes appears to be less modulated and more stereotyped than biting or ram feeding (Aerts, 1990; Aerts and De Vree, 1993; Motta et al., 2002; Robinson and Motta, 2002; Gibb and Ferry-Graham, 2005; Matott et al., 2005), perhaps due to the physical properties of water that demand such rapid and tightly coordinated expansion of the feeding apparatus in order to effectively entrain the prey.

Function and Performance

Despite these functional differences in suction generation, *Ginglymostoma cirratum* generated among the largest recorded suction pressures for any aquatic vertebrate to date (Lauder, 1980a; Lauder and Schaffer, 1985; Grubich and Wainwright, 1997; Ferry-Graham and Lauder, 2001; Sanford and Wainwright, 2002; Svanback et al., 2002; Carroll, 2004; Dean and Motta, 2004b; Wilga et al., 2007). Peak subambient pressure for *G. cirratum* approached, and in one case exceeded negative one atmosphere (−101 kPa). Our largest recorded subambient pressure (−110 kPa) was similar to the mechanically recorded suction pressures of −94 kPa for *G. cirratum* (Tanaka, 1973). These values are also similar to those obtained for the obligate suction-feeding bambooshark *Chiloscyllium plagiosum*, which had a maximum suction pressure of −102 kPa when recorded from catheters implanted inside the buccal cavity (Wilga et al., 2007). However, both *G. cirratum* and *C. plagiosum* do not capture prey any farther, absolutely, from their mouth than do suction-feeding bony fishes that generally generate subambient pressures of −10 to −20 kPa (Svanback et al., 2002; Day et al., 2005; Higham et al., 2005; Nauwelaerts et al., 2006; Westneat, 2006; Wilga et al., 2007). These similar peak values also indicate that the method of pressure recording by the catheter inside the PVC pipe apparently did not adversely affect the pressure values.

The cavitation threshold of sea water on a wettable surface such as the shark's mouth occurs at approximately −56 kPa (Smith, 1991, 1996). On the basis of the subambient pressures measured, the large "popping" sounds that often accompany *Ginglymostoma cirratum* feeding (Motta et al., 2002) are most likely caused by cavitation, and the extremely large forces that occur during cavitation (Versluis et al., 2000) may kill or tear apart prey.

The dominant force that suction-feeding fishes exert on their prey is the fluid pressure gradient experienced by the prey (Wainwright and Day, 2007). The forces exerted on the prey can be elevated by increasing the rate of expansion and/or by reducing the size of the mouth aperture (Muller et al., 1982; Grubich and Wainwright, 1997; Wainwright et al., 2001; Sanford and Wainwright, 2002; Svanback et al., 2002; Carroll et al., 2004; Van Wassenbergh et al., 2006; Wainwright and Day, 2007). In *Ginglymostoma cirratum* peak suction pressure was negatively correlated with the time to reach peak subambient pressure. In other words, the faster peak subambient pressure was reached, the greater the pressure drop. Although

the relative timing of mouth opening and hyoid movement was not recorded in the semicaptive sharks, faster buccopharyngeal expansion is presumably related to a shorter time to reach maximum subambient pressure. Faster strikes also produce the largest and fastest pressure drops in the largemouth bass *Micropterus salmoides* (Svanback et al., 2002), and faster strikes (time to peak mouth opening) are positively related to water flow velocities into the mouth of bluegill sunfish *Lepomis macrochirus* (Day et al., 2005). For both species, minimal buccal pressure occurs when the rate of percent volume change in the buccal cavity is highest, and peak mouth opening occurs after peak subambient pressure in this fish (Sanford and Wainwright, 2002; Day et al., 2005).

In *Ginglymostoma cirratum*, peak mouth opening coincided (1 ± 3 ms after) with peak hyoid pressure; however, peak buccal pressure occurred 12 ms after maximum mouth opening. The maximum rate of buccopharyngeal volume expansion presumably occurs after mandibular depression stops and the hyoid and branchial apparatus continue to depress. Coracoarcualis and coracobranchiales activity occurs for a prolonged period (~100 ms) after maximum mouth opening (Fig. 6 and Matott et al., 2005). It therefore appears that, as in bony fishes, hyoid depression continues to occur after peak subambient pressure is reached and food is drawn into the mouth, resulting in the anterior to posterior flow of water out of the gill slits. Peak buccal pressure was on average slightly greater (9 kPa) than peak hyoid pressure due to the narrow aperture of the mouth compared to the buccopharyngeal cavity (Vogel, 2003). However, these data must be qualified by the fact that the location of the external pressure transducer was not always at a constant location in the buccal cavity due to the nature of the experiment, and slight occlusion of the mouth by the PVC pipe could result in increased flow velocity and consequently larger subambient pressures at the mouth.

Scaling of suction pressure with body size has been controversial—data from bony fishes showing no scaling with size while sharks show an increase in subambient pressure with size (but see Van Wassenbergh et al., 2005; Ramsay and Wilga, 2006; Wainwright et al., 2006; Lowry and Motta, 2007b; Wilga et al., 2007). Our data from the nurse shark match theoretical and empirical results from bony fishes, as peak subambient pressure was not related to total length. From 71 to 244 cm TL *Ginglymostoma cirratum* showed isometric growth of the head and muscles involved with suction feeding and there was no change in maximal angular excursions or gape cycle times (Robinson and Motta, 2002). This suggests that the anatomy and function of the nurse shark feeding apparatus does not change with size. This relationship can be summarized as such—suction pressure is force over area; force scales with the cross sectional area of muscle, which grows with length squared. The area over which the force is exerted also grows with length squared and so their ratio does not grow with length. The largemouth bass *Micropterus salmoides* also maintains isometry in many variables through ontogeny and there is no general scaling effects on pressure (Richard and Wainwright, 1995; Carroll et al., 2004). Peak suction pressure is predicted by the rate of buccopharyngeal expansion in *G. cirratum* rather than shark size. Furthermore, the distance the food was sucked into the mouth in *G. cirratum* was not related to the length of the shark. Differences in satiation could contribute to the conflicting results among these experiments. In bony fishes suction pressure magnitudes vary with predator motivation (Ferry-Graham and Lauder, 2001) and both strike kinematics and suction pressure are inversely related to satiation (Lauder, 1980b; Sass and Motta, 2002).

In fishes, the buccal pressure generated during suction feeding is often used as a measure of prey capture performance. However, this indirect measure of performance does not provide any direct indication of the effect of suction on the prey item. Greater suction pressure does not necessarily mean prey can be sucked from further away (Wainwright et al., 2001; Ferry-Graham et al., 2002; Svanback et al., 2002; Van Wassenbergh et al., 2006). Despite generating large suction pressure, *Ginglymostoma cirratum* has to approach its food very closely to capture it, with a maximum effective suction distance of about 3 cm. The velocity of water flow into the mouth of a suction-feeding fish is directly related to the rate of buccal expansion and falls exponentially with distance from the mouth (proportional to the distance^{-3}). The maximum theoretical distance water may be sucked in by a bony fish has been estimated at approximately one mouth width or 3 cm (Muller et al., 1982; Van Leeuwen and Muller, 1984; Svanback et al., 2002). Empirical tests demonstrate that suction is effective over a distance of approximately one mouth width in fishes. Consequently, prey can be sucked in from a distance of 1.8 cm in front of the mouth in bluegill sunfish *Lepomis macrochirus*, 2.5 cm in the largemouth bass *Micropterus salmoides*, and 2.2 cm in the suction feeding orectolobid bambooshark *Chilosyllium plagiosum* (TL 16–44 cm) (Svanback et al., 2002; Ferry-Graham et al., 2003; Day et al., 2005; Higham et al., 2005; Nauwelaerts et al., 2006; Lowry and Motta, 2007b). Despite considerable differences in body size it appears that sharks and bony fishes are functionally convergent in terms of effective suction distance. The pressure gradient in *C. plagiosum* drops off exponentially with distance from the mouth, falling to near zero within one mouth width (Nauwelaerts et al., 2006; Wilga

et al., 2007), presumably as it does with *G. cirratum*. These sharks generate among the highest recorded subambient pressures of any aquatic-feeding vertebrate. Because the largest force acting on prey during suction feeding is the pressure gradient (Wainwright and Day, 2007), these orectolobid sharks must employ these large pressure gradients to engulf prey of relatively large mass including crabs and bony fishes, some of which may be attached to the substrate (Gudger, 1921; Bigelow and Schroeder, 1948; Castro, 2000; Compagno, 2001).

The suite of morphological and functional characters that make *Ginglymostoma cirratum* a suction specialist (Motta and Wilga, 1999; Motta et al., 2002; Wilga et al., 2007) may constrain its prey capture behavior and prey size, but not its taxonomic prey base. Because *G. cirratum* must approach its prey very closely for suction prey capture to be effective, we suspect it is most effective as an ambush or stalking predator, particularly while hunting at night, or by cornering its prey within reef crevices (Cover illustration). Its reliance on olfactory gradient, when searching for food, would render it particularly effective at nocturnal foraging (Hodgson and Mathewson, 1971; Mathewson and Hodgson, 1972). Suction-feeding sharks like the nurse shark may overcome the constraint of small suction distance by using the substrate or crevices to focus the flow of water into the mouth. Feeding near the substrate (< 1 mouth width), particularly when combined with a long pre-oral snout, extends the effective suction distance by up to 2.5 times for the suction specialist *Chilosyllium plagiosum* (Nauwelaerts et al., 2006) and apparently also for the benthic suction-feeding *Triakis semifasciata* (Lowry and Motta, 2007a). Although there was no apparent increase in suction distance for large or small pieces of food in *G. cirratum* with distance from the substrate, the data are inconclusive because of small sample size. Feeding in or around crevices and the bottom by *G. cirratum* might account for the large number of nocturnally foraging grunts (Haemulidae) captured in south Florida waters (Castro, 2000), as well as the inclusion of relatively small benthic crustaceans and fishes in its diet (Gudger, 1921; Bigelow and Schroeder, 1948; Castro, 2000; Compagno, 2001). Though the reduced dentition and small mouth size make suction more effective, they make prey processing more difficult. It seems that *G. cirratum* co-opts its powerful suction generating capability when processing prey by utilizing a spit-and-suck behavior and head shaking to dismember larger and more durophagous prey that can fit in its mouth (Motta et al., 2002; Matott et al., 2005). Therefore, behavioral specializations can overcome functional constrains in the feeding of *G. cirratum*.

ACKNOWLEDGMENTS

We are greatly indebted to the host of volunteers that helped in these experiments, to Mote Marine Laboratory, the Florida Institute of Oceanography, the Keys Marine Laboratory, St. Lucie Nuclear Power Plant staff, and to Cheryl Wilga for guidance and assistance.

LITERATURE CITED

Aerts P. 1990. Variability of the fast suction feeding process in *Astatotilapia elegans* (Teleostei: Cichlidae): A hypothesis of peripheral feedback control. J Zool Lond 220:653–678.

Aerts P, De Vree F. 1993. Feeding performance and muscular constraints in fish. J Exp Biol 177:129–147.

Baumgartner JV. 1992. Spatial variation of morphology in a freshwater population of threespine stickleback, *Gasterosteus aculeatus*. Can J Zool 70:1140–1148.

Bigelow HB, Schroeder WC. 1948. Fishes of the Western North Atlantic: Lancelets, cyclostomes, sharks. Mem Sears Found Mar Res 2:1–576.

Carroll AM. 2004. Muscle activation and strain during suction feeding in the largemouth bass *Micropterus salmoides*. J Exp Biol 207:983–991.

Carroll AM, Wainwright PC, Huskey SH, Collar DC, Turingan RG. 2004. Morphology predicts suction feeding performance in centrarchid fishes. J Exp Biol 207:3873–3881.

Castro JI. 2000. The biology of the nurse shark, Ginglymostoma cirratum, off the Florida east coast and the Bahama Islands. Environ Biol Fish 58:1–22.

Compagno LJV. 2001. Sharks of the world. An annotated and illustrated catalogue of shark species known to date, Vol. 2. Bullhead, mackerel and carpet sharks (Heterodontiformes, Lamniformes and Orectolobiformes). FAO Species Catalogue for Fishery Purposes. No. 1. Rome, FAO. 269 p.

Compagno L, Dando M, Fowler S. 2005. Sharks of the World. Princeton: Princeton University Press. 368 p.

Day SW, Higham TE, Cheer AY, Wainwright PC. 2005. Spatial and temporal flow patterns during suction feeding of bluegill sunfish (*Lepomis macrochirus*) by particle image velocimetry. J Exp Biol 208:2661–2671.

Dean M, Motta PJ. 2004a. Anatomy and functional morphology of the feeding apparatus of the lesser electric ray, *Narcine brasiliensis* (Elasmobranchii: Batoidea). J Morphol 262:462–483.

Dean M, Motta PJ. 2004b. Feeding behavior and kinematics of the lesser electric ray, *Narcine brasiliensis* (Elasmobranchii: Batoidea). Zoology 107:171–189.

Edmonds MA, Motta PJ, Hueter RE. 2001. Food capture kinematics of the suction feeding horn shark, *Heterodontus francisci*. Environ Biol Fish 62:415–427.

Ferry-Graham LA. 1998. Effects of prey size and mobility on prey-capture kinematics in leopard sharks *Triakis semifasciata*. J Exp Biol 201:2433–2444.

Ferry-Graham LA. 1999. Mechanics of ventilation in swell-sharks, *Cephaloscyllium ventriosum* (Scyliorhinidae). J Exp Biol 202:1501–1510.

Ferry-Graham LA, Lauder GV. 2001. Aquatic prey capture in ray-finned fishes: A century of progress and new directions. J Morphol 248:99–119.

Ferry-Graham LA, Bolnick DI, Wainwright PC. 2002. Using functional morphology to examine the ecology and evolution of specialization. Integ Comp Biol 42:265–277.

Ferry-Graham LA, Wainwright PC, Lauder GV. 2003. Quantification of flow during suction feeding in bluegill sunfishes. Zoology 106:159–168.

Gibb AC, Ferry-Graham LA. 2005. Cranial movements during suction feeding in teleost fishes: Are they modified to enhance suction production? Zoology 108:141–153.

Grubich JR, Wainwright PC. 1997. Motor basis of suction feeding performance in largemouth bass, *Micropterus salmoides*. J Exp Zool 277:1–13.

Gudger EW. 1921. Notes on the morphology and habits of the nurse shark, *Ginglymostoma cirratum*. Copeia 1921:57–59.

Higham TE, Day SW, Wainwright PC. 2005. Sucking while swimming: Evaluating the effects of ram speed on suction generation in bluegill sunfish *Lepomis macrochirus* using digital particle image velocimetry. J Exp Biol 208:2653–2660.

Hodgson ES, Mathewson RF. 1971. Chemosensory orientation in sharks. Ann New York Acad Sci 188:175–182.

Huber DR, Weggelaar CL, Motta PJ. 2006. Scaling of bite force in the blacktip shark *Carcharhinus limbatus*. Zoology 109: 109–119.

Lauder GV. 1979. Feeding mechanisms in primitive teleosts and in the halecomorph fish *Amia calva*. J Zool Lond 187:543–578.

Lauder GV. 1980a. Hydrodynamics of prey capture by teleost fish. Biofluid Mech 2:161–181.

Lauder GV. 1980b. The suction feeding mechanism in sunfishes (Lepomis): An experimental analysis. J Exp Biol 88:49–72.

Lauder GV. 1985. Aquatic feeding in lower vertebrates. In: Hildebrand M, Bramble DM, Liem KF, Wake DB, editors. Functional Vertebrate Morphology. Cambridge: Harvard Press. pp 210–229.

Lauder GV, Shaffer HB. 1985. Functional morphology of the feeding mechanism in aquatic ambystomatid salamanders. J Morphol 185:297–326.

Lowry D, Motta PJ. 2007a. Ontogeny of feeding behavior and cranial morphology in the whitespotted bambooshark *Chiloscyllium plagiosum*. Mar Biol 151:2013–2023.

Lowry D, Motta PJ. 2007b. Relative importance of growth and behavior to elasmobranch suction feeding performance over early ontogeny. J R Soc Interface 1–12. DOI: 10.1098/rsif.2007.1189

Lowry D, Motta PJ, Hueter RE. 2007. The ontogeny of feeding behavior and cranial morphology in the leopard shark *Triakis semifasciata* (Girard 1854): A longitudinal perspective. J Exp Mar Biol Ecol 341:153–167.

Mathewson RF, Hodgson ES. 1972. Klinotaxis and rheotaxis in orientation of sharks toward chemical stimuli. Comp Biochem Physiol Part A 42:79–84.

Matott MP, Motta PJ, Hueter RE. 2005. Modulation in feeding kinematics and motor pattern of the nurse shark *Ginglymostoma cirratum*. Environ Biol Fish 74:163–174.

Moss SA. 1965. The feeding mechanisms of three sharks: *Galeocerdo cuvier* (Peron & Le Sueur), *Negaprion brevirostris* (Poey), and *Ginglymostoma cirratum* (Bonaterre). Ph.D. Dissertation, Cornell University.

Moss SA. 1977. Feeding mechanisms in sharks. Am Zool 17:355–364.

Motta PJ. 2004. Prey capture behavior and feeding mechanics of elasmobranchs. In: Carrier JC, Musick JA, Heithaus MR, editors. Biology of Sharks and Their Relatives. Boca Raton: CRC Press. pp 165–202.

Motta PJ, Wilga CD. 1995. Anatomy of the feeding apparatus of the lemon shark, *Negaprion brevirostris*. J Morphol 226:309–329.

Motta PJ, Wilga CD. 1999. Anatomy of the feeding apparatus of the nurse shark, *Ginglymostoma cirratum*. J Morphol 241:1–29.

Motta PJ, Tricas TC, Hueter RE, Summers AP. 1997. Feeding mechanism and functional morphology of the jaws of the lemon shark *Negaprion brevirostris* (Chondrichthyes, Carcharhinidae). J Exp Biol 200:2765–2780.

Motta PJ, Hueter RE, Tricas TC, Summers AP. 2002. Kinematic analysis of suction feeding in the nurse shark *Ginglymostoma cirratum* (Orectolobiformes, Ginglymostomidae). Copeia 2002: 24–38.

Muller M, Osse JWM, Verhagen JHG. 1982. A quantitative hydrodynamic model of suction feeding in fish. J Theor Biol 95:49–79.

Nauwelaerts S, Wilga C, Sanford C, Lauder G. 2006. Hydrodynamics of prey capture in sharks: Effects of substrate. J Roy Soc Inter 4:341–345.

Osse JWM. 1969. Functional morphology of the head of the perch (*Perca fluviatilis* L.): An electromyographic study. Neth J Zool 19:289–392.

Ramsay JB, Wilga CD. 2006. Anatomy and Functional Morphology of the Feeding Apparatus of White-Spotted Bamboo Sharks, *Chiloscyllium plagiosum*. Abstracts and Programme. New Orleans, LA: American Society of Ichthyologists and Herpetologists.

Ramsay JB, Wilga CD. 2007. Morphology and mechanics of the teeth and jaws of white-spotted bamboo sharks (*Chiloscyllium plagiosum*). J Morphol 268:664–682.

Ramsay JB, Wilga CD. 2008. Adductor Muscle Function During Suction and Biting in Bamboo Sharks. Abstracts. San Antonia, TX: Society for Integrative and Comparative Biology.

Richard BA, Wainwright PC. 1995. Scaling the feeding mechanism of largemouth bass (*Micropterus salmoides*): Kinematics of prey capture. J Exp Biol 198:419–433.

Robinson MP, Motta PJ. 2002. Patterns of growth and the effects of scale on the feeding kinematics of the nurse shark (*Ginglymostoma cirratum*). J Zool Lond 256:449–462.

Sanford CP, Wainwright PC. 2002. Use of sonomicrometry demonstrates the link between prey capture kinematics and suction pressure in largemouth bass. J Exp Biol 205:3445–3457.

Sasko DE, Dean MN, Motta PJ, Hueter RE. 2006. Prey capture and kinematics of the Atlantic cownose ray, *Rhinoptera bonasus*. Zoology 109:171–181.

Sass GG, Motta PJ. 2002. The effects of satiation on prey capture kinematics in the largemouth bass, *Micropterus salmoides*. Environ Biol Fish 65:441–454.

Shirai S. 1996. Phylogenetic interrelationships of *Neoselachians* (Chondrichthyes: Euselachii). In: Stiassny MLJ, Parenti LR, Johnson GD, editors. Interrelationships of Fishes. New York: Academic Press. pp 9–43.

Smith AM. 1991. Negative pressure generated by octopus suckers: A study of the tensile strength of water in nature. J Exp Biol 157:257–271.

Smith AM. 1996. Cephalopod sucker design and the physical limits to negative pressure. J Exp Biol 199:949–958.

Svanback R, Wainwright PC, Ferry-Graham LA. 2002. Linking cranial kinematics, buccal pressure, and suction feeding performance in largemouth bass. Physiol Biochem Zool 75:532–543.

Tanaka SK. 1973. Suction feeding by the nurse shark. Copeia 1973:606–608.

Van Leeuwen JL, Muller M. 1984. Optimum sucking techniques for predatory fish. Trans Zool Soc Lond 37:137–169.

Van Wassenbergh S, Aerts P, Herrel A. 2005. Scaling of suction feeding kinematics and dynamics in the African catfish *Clarias gariepinus*. J Exp Biol 208:2103–2114.

Van Wassenbergh S, Aerts P, Herrel A. 2006. Hydrodynamic modeling of aquatic suction performance and intra-oral pressures: Limitation for comparative studies. J Roy Soc Inter 3:507–514.

Versluis M, Schmitz B, von der Heydt A, Lohse D. 2000. How snapping shrimp snap: Through cavitating bubbles. Science 289:2114–2117.

Vogel S. 2003. Comparative Biomechanics: Life's Physical World. Princeton: Princeton University Press. 580 p.

Wainwright PC, Day SW. 2007. The forces exerted by aquatic suction feeders on their prey. J Roy Soc Inter 4:553–560.

Wainwright PC, Ferry-Graham LA, Waltzek TB, Hulsey CD, Carroll AM, Svanback R. 2001. Evaluating suction feeding performance in fishes. Am Zool 41:1617–1617.

Wainwright PC, Huskey SH, Turingan RG, Carroll AM. 2006. Ontogeny of suction feeding capacity in snook, *Centropomus undecimalis*. J Exp Zool 305A:246–252.

Westneat MW. 1990. Feeding mechanics of teleost fishes (Labridae): A test of four-bar linkage models. J Morphol 205:269–295.
Westneat MW. 2006. Skull biomechanics and suction feeding in fishes. In: Shadwick RE, Lauder GV, editors. Fish Biomechanics. New York: Academic Press. pp 29–75.
Wilga CD. 2008. Evolutionary Divergence in the Suction Feeding Mechanism of Fishes. Abstracts. San Antonia, TX: Society for Integrative and Comparative Biology.
Wilga CD, Motta PJ. 1998. Conservation and variation in the feeding mechanism of the spiny dogfish *Squalus acanthias*. J Exp Biol 201:1345–1358.
Wilga CD, Motta PJ. 2000. Durophagy in sharks: Feeding mechanics of the hammerhead *Sphyrna tiburo*. J Exp Biol 203:2781–2796.
Wilga CD, Lauder GV. 2001. Functional morphology of the pectoral fins in bamboo sharks, *Chiloscyllium plagiosum*: Benthic vs. pelagic station-holding. J Morphol 249:195–209.
Wilga CD, Motta PJ, Sanford CP. 2007. Evolution and ecology of feeding in elasmobranchs. Integ Comp Biol 47:55–69.
Wu EH. 1994. Kinematic analysis of jaw protrusion in orectolobiform sharks: A new mechanism for jaw protrusion in elasmobranchs. J Morphol 222:175–190.